JOURNAL OF MOLECULAR SPECTROSCOPY 77, 298–309 (1979)

High Resolution Spectroscopy of Vibrationally Excited $^{13}CH_3OH$ by Frequency Measurement of FIR Laser Emission[1]

J. O. HENNINGSEN AND J. C. PETERSEN

Physics Laboratory I, H. C. Ørsted Institute, University of Copenhagen, Copenhagen, Denmark

AND

F. R. PETERSEN, D. A. JENNINGS, AND K. M. EVENSON

Laser Metrology Section, National Bureau of Standards, Boulder, Colorado 80302

High resolution spectroscopic data on vibrationally excited $^{13}CH_3OH$ have been obtained by combining the technique of optically pumped FIR lasers with accurate frequency measurements. The frequencies of 20 torsion–rotation transitions in the $C-O$ stretch fundamental were measured and spectroscopically assigned. From these measurements, $^{13}CH_3OH$ molecular constants were determined.

INTRODUCTION

In conventional FIR spectroscopy of molecules, the resolution attainable is typically of the order of 0.1 cm^{-1}, corresponding to a relative accuracy of 10^{-2} to 10^{-3}. The present paper reports on a technique combining the principle of optically pumped laser action in the FIR (*1*) with accurate emission frequency measurements (*2*) making spectroscopy with a Doppler limited resolution of about 10^{-7} possible for certain molecules. The molecules under consideration are those which have a strong, infrared active, vibrational band overlapping the spectrum of an IR laser, typically a CO_2 laser. Normally, in such a case, there will be a number of coincidences that are close enough (within about 50 MHz) that a modestly powered pump laser can, by resonant absorption, transfer a sizable number of molecules from a level J in the ground state to J' in the excited vibrational state, as indicated in Fig. 1. This absorption may create population inversion between the pumped level and the levels below, and when the pumping takes place in a resonator with suitably small losses, stimulated emission may occur on the transitions labeled *a*, *b*, and *c* in Fig. 1. If the lasing is sufficiently intense, inversion may subsequently be created between lower levels $J' - 1$, $J' - 2$, etc., leading to so-called cascade transitions. Also, the initial level may be depleted to such a degree that inversion is created between this

[1] Work supported by the Danish Natural Science Research Council under Grant No. 511-1787.

0022-2852/79/090298-12$02.00/0

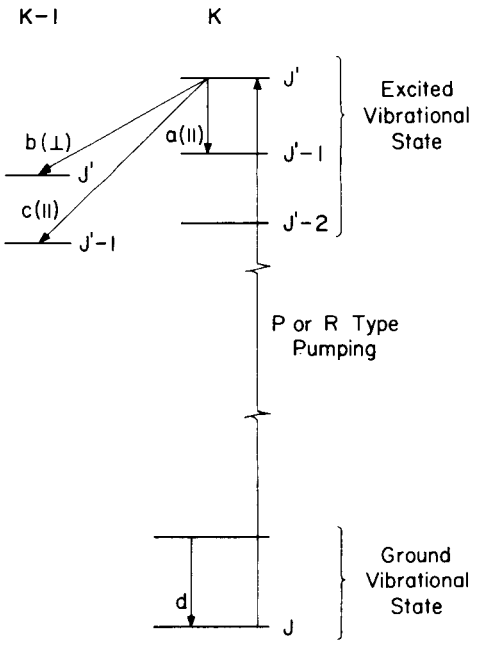

FIG. 1. Principle of optically pumped FIR lasers showing dominant emission lines in CH_3OH laser. The polarization is indicated relative to that of the pump radiation.

level and the one immediately above, leading to refilling transitions in the vibrational ground state such as *d* in Fig. 1.

For near resonant pumping at pressures above a few millitorr (1 Torr = 133 Pascal) maximum gain occurs at the line center of the corresponding transition (for off resonance pumping, the gain for stimulated Raman scattering may become larger than the laser gain, and the FIR signal will then be detuned with respect to the transition frequency (*3*)). The long term fractional frequency instability is basically determined by the mechanical construction of the FIR laser cavity and can easily be made less than 10^{-7} over periods of minutes without active stabilization. Thus, if the emission frequency can be measured accurately, high precision spectroscopic information can be obtained.

A list of molecules which have been used for optical pumping has been published by Yamanaka (*4*), and a periodically updated table is being compiled at the National Physical Laboratory, UK (*5*). The candidate chosen for the present work, $^{13}CH_3OH$, has not previously been studied in this context, and the choice is motivated in several ways. Normal methyl alcohol, together with all its isotopic varieties, is well suited for optical pumping since the C–O stretch fundamental overlaps the CO_2 laser spectrum. Furthermore, because of the hindered internal rotation, the methanols have a particularly rich and extensive FIR spectrum. No transitions have been previously reported in the vibrationally excited $^{13}CH_3OH$ molecule; however, it is sufficiently similar to $^{12}CH_3OH$ that data for this molecule serve as a valuable guideline.

TABLE I

Measured and Calculated Frequencies in $^{13}CH_3OH$ and Their Identification

$^{12}C^{16}O_2$ Pump Line	Line No.	λ (μm)	Measured Frequency (MHz)	λ^{-1}_{meas} [d] (cm^{-1})	$\lambda^{-1}_{calc} - \lambda^{-1}_{meas}$ (cm^{-1})	Pol.	Assignment (nτK),J →(n'τ'K'),J'	Type
$R_{10}(16)$	1	268.6	1 116 245.5	37.233 941	-0.0019	∥	(027),24→(027),23	direct
	2	280.22	1 069 853.4	35.686 468	0.0006		(027),23→(027),22	cascade
	3(b)	-	-	(37.231 172)[b]	0.0027		(036),24→(036),23	combination
	4	280.24	1 069 771.4	35.683 733	0.0054		(036),23→(036),22	cascade
	5(b)	-	-	(37.233 255)[b]	-0.0037		(015),24→(015),23	combination
	6(b)	-	-	(35.688 807)[b]	-0.0029		(015),23→(015),22	combination
	7	203.6	1 472 199.3	49.107 282	-0.0273	⊥	(027),24→(036),24	direct
	8(c)	115.8	2 588 361.7	86.338 454	-0.0246	∥	(027),24→(036),23	direct
	9	332.6	901 351.2	30.065 840	0.0813		(036),24→(015),24	cascade
	10	148.6	2 017 576.1	67.299 095	0.0775		(036),24→(015),23	cascade
	11	152.1	1 971 337.2	65.756 730	0.0718		(036),23→(015),22	cascade
$P_9(10)$	12	208.4	1 438 460.3	47.981 871	-0.0195	∥	$(113),31^-\rightarrow(113),30^-$	direct
	13	146.1	2 052 004.1	68.447 488	-0.466	⊥	$(113),31^-\rightarrow(122),31^+$	direct
	14	86.1	3 481 433.1	116.128 108	-0.607	∥	$(113),31^-\rightarrow(122),30^-$	direct
	15(b)	-	-	(47.680 620)[b]	-0.1414		$(122),31^+\rightarrow(122),30^-$	combination
$P_9(12)$	16(c)	238.5	1 256 871.9	41.924 735	0.0061	∥	$(034),27^-\rightarrow(034),26^-$	direct
	17(c)	461.4	649 766.6	21.673 881	0.0051	⊥	$(034),27^-\rightarrow(013),27^+$	direct
	18(c)	157.9	1 898 279.9	63.319 802	-0.0350	∥	$(034),27^-\rightarrow(013),26^-$	direct
	19(b)	-	-	(41.645 921)[b]	-0.0400		$(013),27^+\rightarrow(013),26^-$	combination
$P_9(22)'$	20	339.0	884 438.0	29.501 678	-0.0161	∥	(019),19→(019),18	direct
	21(c)	149.3	2 008 360.1	66.991 682	-0.1651	⊥	(019),19→(028),19	direct
	22(c)	103.5	2 897 082.4	96.636 268	-0.3177	∥	(019),19→(028),18	direct
	23(b)	-	-	(29.644 586)[b]	-0.1526		(028),19→(028),18	combination
$P_9(22)''$	24(a)	307.8		32.49 [a]	0.00	∥	(1310),21→(1310),20	direct
	25(c)	118.0	2 540 331.0	84.736 321	0.553	⊥	(1310),21→(119),21	direct
	26(c)	85.3	3 513 853.4	117.209 532	0.565	∥	(1310),21→(119),20	direct
	27(b)	-	-	(32.473 211)[b]	0.0125		(119),21→(119),20	combination

a only wavelength measured
b not observed as laser emission
c lines which are particularly strong
d Except for combination lines, from measured frequency with $c = 2.99792458 \times 10^8$ m/s. Combination lines from assignment and differences between measured lines.

EXPERIMENTAL DETAILS

The experiments were carried out in two stages. In the first, an experimental arrangement as previously described was used (*6, 7*). It employs an open-structure FIR resonator pumped by a prism-controlled, 1.2-m-long CO_2 laser capable of delivering 6 W cw and about 30 W in an internally chopped mode. The absorption coincidences in $^{13}CH_3OH$ were detected as a function of CO_2 tuning by a spectrophonic technique employing a microphone mounted in the FIR resonator. FIR laser emission was achieved by length tuning the FIR resonator and detected with a He-cooled Ge(Ga) detector. The wavelengths of the FIR lines were then measured with fractional uncertainties of 3×10^{-4} by using the resonator as a scanning Fabry–Perot interferometer.

In the second stage, the frequencies were measured, and the results are given in Table I. The FIR laser used a 14-mm-i.d. copper waveguide 2 m long and was pumped by a 30-W, 3-m-long cw CO_2 laser. With two frequency stabilized CO_2 lasers, supplemented at times by a stabilized X-band klystron, any frequency throughout the FIR can be synthesized in a W–Ni point-contact diode (*2*). Mixing such a synthesized frequency with the FIR signal in the same point-contact diode produces a beat note inside the 0.1–1500-MHz frequency range of a spectrum analyzer. The frequency of the FIR laser was set to the center of the gain curve with a fractional uncertainty of 3×10^{-7} by observing the beat note on the spectrum analyzer as the laser was tuned. The CO_2 frequencies are known to an accuracy of about 0.03 MHz, and the klystron frequency was measured to within 0.01 MHz. Thus, the overall fractional uncertainty (estimated one sigma) of the FIR frequency determination is about 3×10^{-7}. It is assumed that pressure and other frequency shifts are small in comparison. The predicted frequency from the wavelength measurement usually resulted in a beat note within the range of the spectrum analyzer.

ASSIGNMENT OF LINES

Methyl alcohol is a weakly asymmetric top with an internal degree of freedom referred to as torsion or internal rotation. For a thorough discussion of its energy level spectrum we refer to Kwan and Dennison (*8*). The energy levels are labeled by the quantum numbers $n\tau K$ and J. They are classified in three symmetry types A, E_1, and E_2 according to the symmetry of their internal rotation state, and the A states for low K are subject to splitting due to the asymmetry of the molecule.

The selection rules for transitions involving the parallel component of the dipole moment are

$$\Delta J = 0, \pm 1 \qquad \text{and} \qquad \Delta K = \Delta n = \Delta \tau = 0.$$

For the perpendicular component, which is associated with the OH group, $\Delta K = \pm 1$ with Δn arbitrary and $\Delta \tau$ fixed so as to preserve internal rotation symmetry. Furthermore, each of the latter transitions has associated with it a P and an R type transition, corresponding to a simultaneous change of $\Delta J = \pm 1$. For Δn even, the split A states obey the rules $\pm \rightarrow \pm$ for $|\Delta J| = 1$ and $\pm \rightarrow \mp$ for $\Delta J = 0$, while the reverse holds for Δn odd.

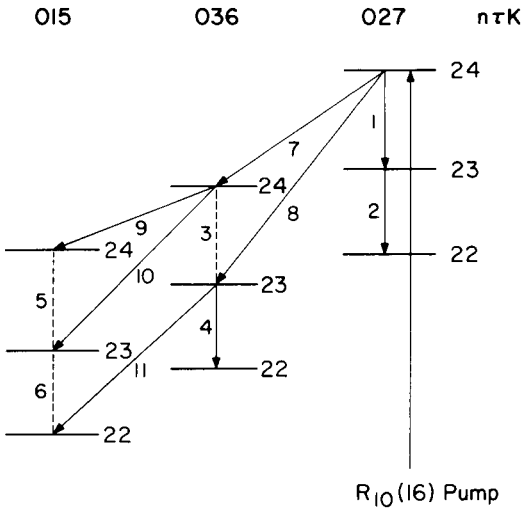

FIG. 2. Observed direct and cascade lines in $^{13}CH_3OH$ pumped by $R_{10}(16)$ of a CO_2 laser. Numbering refers to Table I.

In conventional spectroscopy, all transitions inside the frequency range considered are recorded. In the present experiment, information is obtained about an essentially randomly selected number of transitions, and the main problem is identification (*9*). Therefore, attention is restricted to cases where a given pump line produces at least three emission lines forming a triad (*a*, *b*, and *c*) as indicated in Fig. 1. Other lines were measured and will be reported elsewhere (*10*). If the FIR resonator is an open structure and is pumped by linearly polarized CO_2 radiation, the FIR radiation will be linearly polarized, parallel to the pump for $\Delta J_1 + \Delta J_2$ even and orthogonal to the pump for $\Delta J_1 + \Delta J_2$ odd (*9*). Here ΔJ_1 and ΔJ_2 are the changes in J caused by the pump transition and the emitting transition, respectively. For any triad, only two of the lines have the same polarization, and the third line is then identified as the Q-branch transition ($\Delta J = 0$). The FIR polarization relative to the pump further identifies the character of the pump transition. With this information at hand, the complete assignment of the $^{13}CH_3OH$ lines can usually be performed by comparison with the well-known $^{12}CH_3OH$ ground state spectrum (*8*, *11*).

OBSERVATION OF CASCADE LINES

The most extensive data were taken with the CO_2 laser tuned to $R_{10}(16)$, with results as listed in Table I and on Fig. 2. In the preliminary experiment only the three direct transitions (1, 7, and 8) were detected. The cascade transitions lase only when the parent transition is simultaneously lasing. Cascade lines are seldom observed in open structure resonators because of the limited number of oscillating modes. The FIR open-structure cavity can be simultaneously resonant on two different frequencies only for very special mirror separations. In a metal waveguide, however, the density of low loss modes is so

large that strong lines oscillate for most mirror separations, and the requirements for oscillation of cascade transitions are often satisfied. A total of five cascade lines were observed, and from combination relations, the frequencies of another three transitions which did not lase could be calculated. Identification of the origin of the cascade lines was done by correlating the presence of the beat note with the total laser output as a function of the FIR resonator length. The beats could be grouped together in sequences with separations typical of either the parent line or the cascade line itself.

MULTIPLE EMISSION

In addition to facilitating the observation of cascade lines, the close spacing of low loss modes of the metallic waveguide has another use. Occasionally, on the spectrum analyzer a beat note was observed which was not related to the synthesizing signals and whose frequency was only weakly dependent on the length tuning of the resonator. In the $R_{10}(16)$ case such a beat note was observed at 84.0 MHz. Inspection of the measured frequencies of Table I shows that the difference between line No. 8 and the sum of Nos. 1 and 7, amounts to 82.6 MHz. The conclusion, therefore, is that all three direct transitions are oscillating simultaneously and mixing in the point-contact diode. This observation serves as a powerful check on the accuracy of the frequency measurements.

A related observation was made when searching for a possible cascade lasing transition, No. 3, Fig. 2. Initially, a beat note was found on the spectrum analyzer at exactly the predicted frequency. However, by dispersive filtering of the FIR signal reaching the diode, the attenuation of the beat note was found to be typical of a much higher frequency. It was therefore concluded that the beat note was synthesized in the diode from transitions No. 7 and 8 lasing simultaneously and that transition No. 3 was not present in the output from the laser. This observation is, in fact, not unexpected since the strong $\Delta J = \Delta K = -1$ transition (No. 8) tends to fill the (036), 23 level and thus counteracts the inversion.

ENERGY LEVELS

The J dependent part of the energy is given by (*8, 11*)

$$\begin{aligned} E(n\tau K,J) = [&\tfrac{1}{2}(B + C) + F_v\langle 1 - \cos 3\gamma\rangle + G_v\langle P_\gamma^2\rangle \\ &+ L_v K\langle P_\gamma\rangle - D_{JK}K^2 + b(n\tau K)]J(J+1) \\ &- [D_{JJ} - d(n\tau K)]J^2(J+1)^2 \\ &+ \text{higher order terms in } J(J+1) \\ &(+A\text{-state splitting}) \end{aligned} \tag{1}$$

where B and C are related to the moments and cross-moments of inertia through

$$B = \frac{I_b}{I_b^2 + I_{ab}^2}\frac{\hbar}{4\pi}, \tag{2}$$

$$C = \frac{1}{I_c}\frac{\hbar}{4\pi}. \tag{3}$$

The next three terms in the square brackets arise from the interaction between internal and external rotation while D_{JK} and D_{JJ} are the usual centrifugal distortion constants. The asymmetry terms $b(n\tau K)$, $d(n\tau K)$, and the A-state asymmetry splitting may be calculated by second order perturbation theory starting out from a symmetric top representation.

The J-independent part of the energy is given by

$$E(n\tau K) = \tfrac{1}{2}V_3\langle 1 - \cos 3\gamma\rangle + F\langle P_\gamma^2\rangle + [A - \tfrac{1}{2}(B + C)]K^2 - D_{KK}K^4 + \tfrac{1}{2}V_6\langle 1 - \cos 6\gamma\rangle + \{7 \text{ Kirtman terms}\}. \quad (4)$$

Here, the first three dominant terms are determined by the height V_3 of the barrier against internal rotation, by

$$F = \frac{I_a I_b - I_{ab}^2}{I_{a1}I_{a2}I_b - I_{a2}I_{ab}^2}\frac{\hbar}{4\pi} \quad (5)$$

TABLE II

Parameters Used for Energy Level Calculations[a]

	$^{12}CH_3OH$, V=0	$^{12}CH_3OH$, V=1	$^{13}CH_3OH$, V=0	$^{13}CH_3OH$, V=1
I_b	34.003856	34.3495	34.8622	35.2553
I_c	35.306262	35.7288	36.1608	36.6382
I_{ab}	-0.1079		-0.123	
I_{a1}	1.2504		1.2528	
I_{a2}	5.3331	5.3486	5.3331	5.3874
V_3	373.21	392.2	372.6	386.8
V_6	-0.52			
D_{KK}	0.38×10^{-4}			
K_1	-0.48×10^{-4}			
K_2	-18.41×10^{-4}			
K_2	-53.73×10^{-4}			
K_4	-85.50×10^{-4}			
K_5	132.07×10^{-4}			
K_6	67.85×10^{-4}			
K_7	0			
F_v	-2.389×10^{-3}		-2.323×10^{-3}	
G_v	-1.168×10^{-4}		-1.127×10^{-4}	
L_v	-2.26×10^{-6}			
D_{JK}	9.54×10^{-6}			
D_{JJ}	1.6345×10^{-6}			

[a] Moments of inertia are in units of kg $\times$ m^2 $\times$ 10^{-47}, and expansion coefficients are in units of cm^{-1}.

TABLE III

Q-Band Expansion Coefficients in Units of cm^{-1}

Q-band		q_0	q_1	q_2	q_3	q_4
$^{13}CH_3OH$, V=0	012←021	0.90281	-0.885×10^{-4}	3.005×10^{-6}	1.121×10^{-8}	-1.634×10^{-10}
$^{13}CH_3OH$, V=1	027←036	49.113	-1.029×10^{-4}	0.0571×10^{-6}	0.0416×10^{-8}	-0.0042×10^{-10}
	036←015	30.163	-1.768×10^{-4}	0.2313×10^{-6}	-0.1097×10^{-8}	0.0125×10^{-10}

where I_a is the moment of inertia about the a axis, I_{a2} is the moment of inertia of the methyl group about its symmetry axis, and $I_{a1} = I_a - I_{a2}$, and by $A - \frac{1}{2}(B + C)$, where

$$A = \left(\frac{I_a + I_b}{I_a I_b - I_{ab}^2} - \frac{I_b}{I_b^2 + I_{ab}^2} \right) \frac{\hbar}{4\pi} . \tag{6}$$

D_{KK} is a centrifugal distortion term, V_6 represents the deviation of the potential from a perfect sinusoid, and the seven Kirtman terms are interaction terms involving combinations of powers of K and various internal rotation matrix elements.

For transitions with $\Delta n = \Delta K = 0$ and $\Delta J = -1$, we get from Eq. (1)

$$\Delta E(n\tau K, J \to J - 1) = 2JB_{\text{eff}}(n\tau K) - 4[D_{JJ} - d(n\tau K)]J^3 + \text{higher order terms in } J \quad (+A \text{ splitting}) \tag{7}$$

and for transitions with $\Delta K \neq 0$, $\Delta J = 0$ from Eq. (4).

$$\Delta E(n\tau K \to n'\tau' K', J) = q_0 + q_1 J(J + 1) + q_2 J^2(J + 1)^2 + q_3 J^3(J + 1)^3 + q_4 J^4(J + 1)^4 + \cdots \tag{8}$$

where $B_{\text{eff}}(n\tau K)$ represents the first square bracket in Eq. (1), and Eq. (8) is referred to as the Q-branch expansion.

DATA ANALYSIS

The amount of data is too restricted to allow a brute force calculation of all the parameters involved in Eqs. (1) and (4) by a least square procedure. We therefore take as adjustable parameters I_b, I_{a2}, and V_3, while the remaining ones are derived from the literature.

Energy levels are calculated with the computer program developed by Kwan and Dennison (*8*). Asymmetry effects are calculated by second order perturbation theory, including coupling up to $n = 3$ torsional levels. The input parameters are listed in Table II, and where nothing is entered, the value is taken as that of the previous column. Column one contains parameters for the vibrational ground state ($v = 0$) of $^{12}CH_3OH$. a-type parameters are from (*11*), assuming $B - C = 910$ MHz (Table II of (*11*)), and b-type parameters are from Table I of (*8*). All moments of inertia are calculated on the basis of $c = 2.99792458 \times 10^8$ m/sec and $h = 6.626196 \times 10^{-34}$ J sec. The difference between I_{a1} and I_{a2} of Table II, and those of Ref. (*8*), arises from a slightly different choice for h. The second

TABLE IV

Measured and Calculated Frequencies for some High-J Q-Band Transitions in $^{12}CH_3OH$

Transition ($n\tau K \rightarrow n'\tau'K'$) J	Measured (cm^{-1})	Calculated (cm^{-1})	Deviation (cm^{-1})
(0210→039)27	60.686	60.590	-0.096
(039→018)30	51.54	60.590	-0.07
(018→027)16	58.625	58.572	-0.053
(034→013)25	21.321	21.386	0.065

column gives the parameters of the C–O stretch state ($v = 1$) of $^{12}CH_3OH$. I_b and I_c are derived from the measured 0.00883 cm^{-1} reduction of the rotational constant (*9, 12*), assuming all the change to be associated with $\frac{1}{2}(B + C)$,[2] and using $B - C = 942.9$ MHz derived from measured A-state splittings (*14*). I_{a2} and V_3 are taken from Woods (*12*). Based on a comparison with the C–F stretch state of CH_3F he estimates an 0.01-cm^{-1} reduction in A, and assuming unchanged I_{a1} he then finds V_3 to be increased by 19 ± 2 cm^{-1}. The parameters I_b, I_c, and I_{ab} for the $^{13}CH_3OH$ ground state are taken directly from Table 8 of (*15*), whereas for I_{a1} and V_3 we take the change induced by the isotopic substitution from (*15*) and add it to our $^{12}CH_3OH$ values. This is appropriate since Kirtman terms are not taken into account in (*15*).

The parameters of the last column are derived from our $R_{10}(16)$ data. We are here dealing with transitions involving rather high J values, and since we cannot in a systematic way incorporate third and fourth order terms in $J(J + 1)$ in our analysis, we shall first estimate the importance of these terms. A number of Q bands have previously been followed to high J and as an example the coefficients for the $012 \rightarrow 021$ transition of $^{13}CH_3OH$, $v = 0$, are given in Table III (*16*). Here, the third and fourth order contributions at $J \gtrsim 20$ are so large that the validity of a power series expansion is questionable. However, the bands studied so far all involve low K, and since the higher order terms arise mainly from the asymmetry, they are expected to become less important as K increases. To quantify this statement we consider four Q-band transitions at high J in the C–O stretch state of $^{12}CH_3OH$ (*9, 17*). Table IV shows the four measured frequencies together with calculated values based on the parameters of Table II, column 2. In all four cases the deviation is less than 0.1 cm^{-1}, and this suggests that $q_3 \lesssim 5 \times 10^{-10}$ cm^{-1} and $q_4 \lesssim 5 \times 10^{-13}$ cm^{-1}.

As initial parameters we choose those of Table II, column 3. Improved values for I_b and I_c are found from the six $K = 0$ transitions, using interaction terms and asymmetry effects for $v = 0$, and assuming $B - C$ to be unchanged. To find I_{a2} and V_3 we use the Q-band transitions ($027 \rightarrow 036 \rightarrow 015$). Referring to the results for $^{12}CH_3OH$ the band origins found by using Eq. (8), neglecting

[2] Lees (*13*) suggests that part of the change in the rotational constant is associated with a significant increase of the interaction constants F_v and G_v. However, since his data did not allow a unique determination of these constants we have chosen to work with the simpler assumption of unchanged F_v and G_v. This does not affect the conclusions drawn from our analysis.

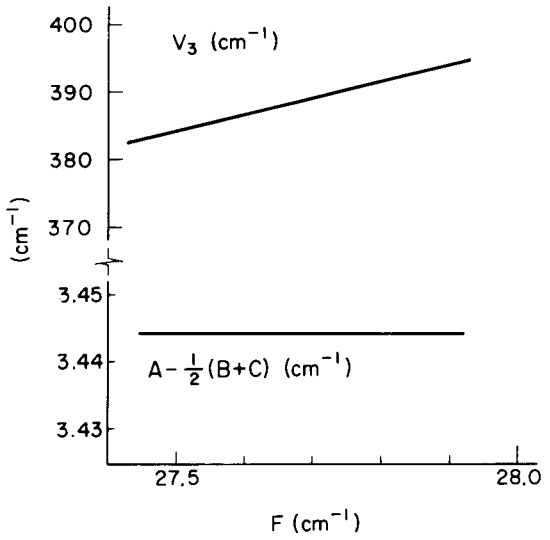

FIG. 3. Parameters V_3 and $A - \frac{1}{2}(B + C)$ as a function of assumed value for F.

third and fourth order terms, and extrapolating to $J = 0$ with calculated q_1 and q_2, are believed to be in error by at most 0.1 cm^{-1}. However, since the transition frequencies are known in each case for three different J values, we have chosen instead to use Eq. (8) with calculated q_1 and q_2, and to solve for q_0, q_3, and q_4. This presumably gives a better value for q_0, and at the same time it provides an independent check on the magnitude of q_3 and q_4. The two band origins are then used with Eq. (4) to determine $\frac{1}{2}V_3$ and $A - \frac{1}{2}(B + C)$ for a range of F values, with all the higher order terms fixed at their $v = 0$ values. The result is shown in Fig. 3, and it is seen that $A - \frac{1}{2}(B + C)$ is essentially independent of the choice of F. If we assume I_{a1} to be unchanged, we can evaluate I_{a2} from Eq. (6) and F from Eq. (5), and hence also find an improved value for V_3 from Fig. 3. The whole procedure is now repeated on the basis of the new set of parameters, and the final result of this iterative procedure appears in column 4 of Table II and in Table III.

Activation of the C–O stretch mode is found to increase I_b and I_c by about 1.1%. This result is similar to that found for $^{12}CH_3OH$ where the increase is 1.0%. The internal rotation barrier V_3 increases by 14.2 cm^{-1} which is somewhat less than the 19 ± 2 cm^{-1} found by Woods (*12*) for $^{12}CH_3OH$, and our value for I_{a2} is about 1.0% higher than the $v = 0$ value, whereas a comparison with $^{12}CH_3OH$ would suggest an 0.3% increase. However, it should be noted that V_3 and I_{a2} for $^{13}CH_3OH$, $v = 0$, have not been determined with the same degree of accuracy as for $^{12}CH_3OH$, $v = 0$.

OTHER PUMP LINES

Four additional pump lines were each found to produce three interrelated emission lines, and the measured frequencies are listed in Table I. The two sets of

lines observed in $P_9(22)$ correspond to two different frequency offsets measured with respect to the CO_2 line center; therefore, they belong to two nearly coincident pump transitions.

The only reasonable assignment for the level pumped by $P_9(12)$ is (034),27. For the $\Delta K = 0$ transition the agreement is satisfactory whereas the excellent agreement for the Q-band transition may be fortuitous in view of the fact that third and fourth order terms are neglected. The $\Delta J = \Delta K = -1$ transition is very sensitive to the A-state asymmetry splitting and the measured frequency corresponds to a value for $B - C$ which is 5% lower than that derived from Table II.

For $P_9(22)'$ the two $\Delta K = 0$ frequencies are also significantly different. However, the difference is not consistent with any A-state splitting, and we can not at present account for this rather large discrepancy.

The remaining two emission line triads have been assigned to transitions in the first excited torsional state $n = 1$. For the $\Delta K = 0$ transitions the agreement is quite good whereas the Q-band transitions deviate by about 0.6 cm^{-1}. A possible explanation may be perturbations caused by the nearly degenerate COH bending mode (*18*).

CONCLUSION

It has been shown that by combining the technique of optically pumped FIR lasers with accurate frequency measurements, high resolution spectroscopic information can be obtained about vibrationally excited molecules. It should be emphasized that a heterodyne technique seems to be the only possible method with sufficient sensitivity and resolving power to observe all the cascade transitions. These are generally weak and appear on a background of very strong signals from the direct lines which are often less than 100 MHz away.

When using conventional spectroscopic techniques a large body of experimental information is needed in order to identify the Q bands, and for vibrationally excited states of CH_3OH only the $012 \rightarrow 021$ transition, which is located in the microwave range, has been observed. With the present technique a number of Q-band frequencies are measured directly with high precision. The main problem is associated with the high J values which require third and fourth order terms to be incorporated in the analysis. In the present case this was made possible by the observation of cascade transitions.

The results of our analysis of $^{13}CH_3OH$ data are generally consistent with known results for $^{12}CH_3OH$. However, we have used a very limited number of measured frequencies, and it has been tacitly assumed that none of the energy levels involved are perturbed by interactions not explicitly incorporated in our model. To verify this, a larger degree of redundancy would be desirable. Additional experimental information could be obtained by pumping with isotopic CO_2 lasers or sequence band CO_2 lasers, but this would still rely on accidental coincidences between pump lines and absorption lines. If, on the other hand, a continuously tunable pump laser of a few watts were available, a completely systematic investigation would be possible, and the excited vibrational bands could then be fully analyzed with unprecedented accuracy.

ACKNOWLEDGMENTS

We wish to thank Dr. Y. Y. Kwan for making a copy of the computer program for energy level calculations available, and Mr. L. Storr-Hansen for extending the program to incorporate asymmetry shifts. One of us (JOH) also wishes to thank the NBS, Boulder, for its hospitality during a two week stay.

REFERENCES

1. T. Y. Chang and T. J. Bridges, *Opt. Commun.* **1,** 423–426 (1970).
2. F. R. Petersen, K. M. Evenson, D. A. Jennings, J. S. Wells, K. Goto, and J. J. Jiménez, *IEEE J. Quantum Electron.* **QE-11,** 838–843 (1975).
3. R. J. Temkin, *IEEE J. Quantum Electron.* **QE-13,** 450–454 (1977).
4. M. Yamanaka, *Rev. Laser Eng.* **3,** 253–294 (1976).
5. D. J. E. Knight, private communication.
6. J. O. Henningsen and H. G. Jensen, *IEEE J. Quantum Electron.* **QE-11,** 248–252 (1975).
7. J. O. Henningsen and J. C. Petersen, "Proceedings of the Third International Conference on Sub-mm Waves and Their Applications," *Infrared Physics.* **18,** 475–479 (1978).
8. Y. Y. Kwan and D. M. Dennison, *J. Mol. Spectrosc.* **43,** 291–319 (1972).
9. J. O. Henningsen, *IEEE J. Quantum Electron.* **QE-13,** 435–441 (1975).
10. F. R. Petersen, D. A. Jennings, K. M. Evenson, and J. O. Henningsen, in preparation.
11. R. M. Lees and J. G. Baker, *J. Chem. Phys.* **48,** 5299–5319 (1968).
12. D. R. Woods, Thesis, University of Michigan, Ann Arbor, 1970.
13. R. M. Lees, *J. Chem. Phys.* **57,** 2249–2252 (1972).
14. J. P. Sattler, T. L. Worchesky, and W. A. Riessler, *Infrared Physics* (to be published).
15. M. C. L. Gerry, R. M. Lees, and G. Winnewisser, *J. Mol. Spectrosc.* **61,** 231–242 (1976).
16. E. V. Ivash and D. M. Dennison, *J. Chem. Phys.* **21,** 1804–1816 (1953).
17. J. O. Henningsen, *IEEE J. Quantum Electron.* **QE-14,** 958–962 (1978).
18. A. Serrallach, R. Meyer, and Hs. H. Günthard, *J. Mol. Spectrosc.* **52,** 94–129 (1974).